Complexes of Th(IV), Zr(IV) and V(IV) with Norfloxacin: Synthesis, Spectroscopic, Thermal, Kinetic Measurements and Antimicrobial Evaluation

Abdel Majid A. Adam
Department of Chemistry, Faculty of Science, Taif University
PO box 888, Taif, Saudi Arabia
Tel: 966-502-099-808 E-mail: majidadam@yahoo.com

Received: November 21, 2011 Accepted: December 6, 2011 Published: January 1, 2012
doi:10.5539/jmsr.v1n1p167 URL: http://dx.doi.org/10.5539/jmsr.v1n1p167

Abstract

M(IV) complexes of thorium, zirconium, and vanadium with norfloxacin were synthesized and characterized with physical and spectroscopic techniques, including elemental analysis (C,H,N), IR, electronic, ^{1}H NMR spectral methods, as well as thermogravimetric (TG) and differential thermogravimetric (DTG) analyses. Based on these studies, the proposed structure of the obtained complexes are $[Th(NFX)_2Cl_4]$, $[Zr(NFX)_2Cl_2]Cl_2$ and $[VO(NFX)_2]SO_4$ (where, NFX: norfloxacin). In all complexes, norfloxacin acts as a bidentate deprotonated ligand bound to the metal through the pyridone and one carboxylate oxygen atoms, forming eight, six, five atoms ring with Th (IV), Zr(IV) and V(IV) metal ions, respectively. The kinetic thermodynamic parameters, such as, activation energy, E^*, enthalpy, ΔH^*, entropy, ΔS^*, and Gibbs free energy, ΔG^*, have been calculated from the TG and DTG curves, using Coats-Redfern and Horowitz-Metzger methods. Norfloxacin as well as their metal complexes were also evaluated for their antibacterial activity against several bacterial species, such as *Bacillus subtilis*, *Pseudomonas aeruginosa* (*P. aeruginosa*), and *Escherichia coli* (*E. coli*) and antifungal screening was studied against three species: *Aspergills flavus*, *Fusarium solani*, and *Penicillium verrcosum* (*P. verrcosum*). The results show significant increase in antibacterial and antifungal activity of metal complexes as compared to the NFX itself.

Keywords: Norfloxacin complexes, Thermal analysis, Kinetic parameters, Antimicrobial evaluation

1. Introduction

Introduction of nalidixic acid during 1962 has shown the new avenue for patients with the bacterial infections and the dramatic impact in altering morbidity and mortality rate compared with the chemotherapy during 1940s. The continuous effort to increase the efficacy against bacteria has led to identify new prototype quinolone, which is active only against Gram-negative bacteria, similar to that of nalidixic acid (Sunduru et al., 2011). However, during 1980s, the introduction of fluoroquinolone drugs has changed the landscape of antibacterial chemotherapy, which was active against both Gram-negative and Gram-positive bacteria pathogens (Koga et al., 1980). Fluoroquinolones are broad-spectrum antibiotics widely used for the treatment of numerous diseases (Reynolds, 1993; Naumann & Dopp, 1989). The most active fluoroquinolone drugs are Norfloxacin, Ciprofloxacin, Sparfloxacin, and Trovafloxacin. The antibacterial activity of fluoroquinolones depends not only on the bicyclic heteroaromatic pharmacophore but also on the nature of the peripheral substituent's and their spatial relationship (Koga et al., 1980;, Fang et al., 2000; Efthimiadou et al., 2007). These substituents exert their influence on antibacterial activity by providing additional affinity for the bacterial enzymes, enhancing the cell penetration, or altering the pharmacokinetics (Chu et al, 1986; Domagala et al, 1988). Norfloxacin (NFX, Fig. 1) (1-ethyl -6-fluoro -4-oxo-7- (1-piperazinyl) -1,4-dihydroquinoline- 3- carboxylic acid) is a second generation fluoroquinolone, and widely used representative member of this family (Dhaneshwar et al, 2001). It is antibiotic agent that extensively used in both human and veterinary medicine (Cui et al., 2011). Norfloxacin (NFX) is active against a wide variety of aerobic Gram-negative and Gram-positive bacteria but specifically, active against aminoglycoside-resistant Pseudomonas aeruginosa and betalactamase producing organisms (Shaikh et al., 2007). When dealing with the interaction between drugs and metal ions in living systems, a particular interest has been given to the interaction of metal ions with antibiotics. Presence of metal ions considerably alters the activity of

fluoroquinolones against potentially susceptible bacteria (Shaikh et al., 2007). A number of works have been reported about the synthesis and characterization of new metal complexes with fluoroquinolone antibacterial agents (Shaikh et al., 2007; Turel et al., 1997a; Turel et al., 1998; Wu et al., 2003; Refat, 2007; Al-Mustafa, 2002; Sadeek et al., 2006; Polk & Pharm, 1989).

In this paper, the interaction of norfloxacin (NFX) with tetraverse transition metal ions in an attempt to examine the mode of norfloxacin coordination and the biological properties of the resulting complexes. In particular, complexes of NFX with the Th(IV), Zr(IV), and V(IV) have been synthesized and characterized with elemental analysis, infrared (IR), 1H NMR and electronic spectra. The thermal behavior of the obtained complexes has also been studied as well as their biological activity against several microorganisms. The antibacterial activity was tested against *Bacillus subtilis*, *Pseudomonas aeruginosa* (*P. aeruginosa*), and *Escherichia coli* (*E. coli*) and antifungal screening was studied against three species: *Aspergills flavus*, *Fusarium solani*, and *Penicillium verrcosum* (*P. verrcosum*).

2. Materials and Methods

2.1 Materials

All chemicals used were of analytical reagent grade, commercially available, and were used without further purification. Egyptian Interactional Pharmaceutical Industrial Company (EIPICO) supplied Norfloxacin used in this work. $Th(NO_3)_4$, $ZrCl_4.xH_2O$, and $VOSO_4.5H_2O$ were purchased from Aldrich Chemical Company.

2.2 Synthesis of the metal complexes

Norfloxacin (2 mmol) in mixed solvent (50/50 %) of methanol/acetone was stirred at room temperature for 20 min. A solution of 1.0 mmol of $Th(NO_3)_4$, $ZrCl_4$, and $VOSO_4$ in 5 ml of methanol was added to the norfloxacin solution with constant stirring. The resulting mixture was heated ~ 50 °C under reflux on a water bath for about 12 h and then cooled. The resulted solid complexes were separated from the reaction mixture by filtration, washed with methanol and dried under vacuum to a constant weight. The yields were found around 70% based on the metal salts. The compounds resulted have low solubility in water and in common organic solvents. The obtained complexes were characterized by their elemental analysis, infrared, electronic, and ^1H NMR, as well as thermal analysis.

2.3 Instrumentation and physical measurements

2.3.1 Elemental analysis

Elemental analysis was performed using a Perkin-Elmer CHN 2400, and the metal contents were found gravimetrically by ignition-weighted samples in atmospheric air to constant weight and definite structure.

Decomposition of complexes was performed in concentrated HNO_3. After decomposition, the sample was diluted with water to 100 ml, and qualitative presence of Cl^- ions (in Th(IV) Zr(IV) complexes), and SO_4^- ions (in V(IV) complex) were determined by means of $AgNO_3$ and $BaCl_2$, respectively.

2.3.2 Molar conductivity

Molar conductivities of freshly prepared 10^{-3} mol dm^{-3} DMSO solutions were measured on a Jenway 4010 conductivity meter.

2.3.3 Electronic spectra

Electronic spectra were recorded in the region of (200-800 nm) for DMSO solution (10^{-3}) of the NFX and their three complexes with Shimadzu UV-spectrophotometer model 1601 PC with a 1 cm quartz cell.

2.3.4 Infrared spectra

Infrared (IR) measurements were carried out on a Genesis II FT-IR spectrophotometer using KBr pellets in the υ= 400-4000 cm^{-1} range.

2.3.5 ^1H NMR spectra

^1H NMR spectra of Thorium complex was obtained on a Varian Gemini 200 MHz spectrometer using DMSO-d6 as solvent and TMS as an internal reference. ^1H NMR data are expressed in parts per million (ppm), referenced internally to the residual proton impurity in DMSO solvent.

2.3.6 Thermal analysis

Thermogravimetric measurements (TG and DTG) were carried out in dynamic nitrogen atmosphere (30 ml/min.) between room temperature and 900 °C with a heating rate of 10 °C/min. using a Shimadzu TGA –50H thermal analyzers.

2.4 Antimicrobial investigation

Antibacterial activity of the Th(IV), Zr(IV), and V(IV) complexes, and the NFX ligand, as well as the pure solvent was investigated by a previously reported modified method of Beecher and Wong (Beecher & Wong, 1994), against different bacterial species, such as *Escherichia coli* (*E. coli*), *Bacillus subtilis*, and *Pseudomonas aeruginosa* (*P. aeruginosa*), and antifungal screening was studied against three species, *Aspergills flavus*, *Fusarium solani*, and *Penicillium verrcosum* (*P. verrcosum*). The microorganisms were purchased from the laboratory of (Microbiology) in the Egyptian International Pharmaceutical Industrial Company (EIPICO).

3. Results and Discussion

The results of the elemental analysis and some physical characteristics of NFX ligand and the obtained complexes are given in Table 1 (Note 1.). The complexes were synthesized using 1:2 (metal: ligand) mole ratio of all reactants. The elemental analysis (Table 1) of the complexes indicates a 1:2 metal to ligand stoichiometry, too. All complexes are stable in air, hygroscopic, with high melting points, insoluble in water, but partly soluble in dimethylformamide; DMF. All complexes have been prepared at high yield (73-76%), and melting points of the complexes are higher than that of the ligand revealing that the complexes are much more stable than ligand. The molar conductance values (Table 1) of the complexes in DMF solvent (10^{-3} mol dm^{-3}) lay in the range of 73.00-87.20 Ω^{-1} cm^2 mol^{-1} (at 25 °C), which indicates that the complexes are electrolytes, and the complexes are of much increasing in electrolytic nature than NFX ligand. The low conductivity values are in agreement with the low solubility of NFX complexes in water, ethanol, chloroform, acetone and most organic solvents. On the other hand, they are soluble in DMSO and DMF. The proposed structures of the obtained complexes are shown in Fig. 2. These structures were confirmed by its analytical data.

3.1 Infrared spectra

The IR spectra of quinolones are most representative in the region 1800-1300 cm^{-1} (Turel et al., 1997b). The tentative assignments of IR bands of Th(IV), Zr(IV), and V(IV) complexes are presented in Table 2 (Note 2. and 3.) and Fig. 3, and have been compared with those of the free ligand norfloxacin, in order to determine the site of coordination that may be involved in chelation.

(i) The IR spectral data of NFX (Table 2) showed two characteristic peaks at 1716 cm^{-1} (characteristic of the $\upsilon(C{=}O)_{carb}$ stretching vibration of the carboxylic group), and 1630 cm^{-1} (attributed to the $\upsilon(C{=}O)_p$ of pyridone keto) (Sadeek, 2005; Sadeek et al, 2009).

(ii) Th(IV), Zr(IV), V(IV) complexes shows no absorption band at ~1700 cm^{-1} $\nu(C{=}O)$, that is indicative of the deprotonation of –COOH group and involvement of the carboxyl group in the formation of Th-O, Zr-O, and V-O bonds.

(iii) The $\upsilon(C{=}O)_p$ peak (of pyridone keto) is shifted from 1630 cm^{-1} in the ligand to lower frequencies in the complexes (~ 1610-1617 cm^{-1}) upon bonding.

(iv) The spectra of the three complexes shows two very strong to strong characteristic bands (~1575 cm^{-1} and ~1380) at 1576-1380, 1579-1382, 1583-1381 cm^{-1} for Th(IV), Zr(IV), V(IV) complexes, respectively, assigned as ν(O-C-O) asymmetric and symmetric stretching vibrations of the ligated carboxylate anion, respectively. These bands are weak in the spectrum of NFX. These complexes also have medium intensity peak around ~1450 cm^{-1} that correspond to asymmetrical and symmetrical carboxylate anion stretching.

Deacon and Phillips, 1980, have studied the criteria that can be used to distinguish between the three binding states of the carboxylate complexes. These criteria are: (a) $\Delta\nu$>200 cm^{-1} (where $\Delta\nu=[\nu as(COO^-)-\nu s(COO^-)]$) this relation was found in case of monodentate carboxylato complexes, (b) bidentate or chelating carboxylato complexes exhibit $\Delta\nu$ significantly smaller than ionic values ($\Delta\nu$<100 cm^{-1}), and finally, (c) bridging complexes show $\Delta\nu$ comparable to ionic values ($\Delta\nu$~150 cm^{-1}). Therefore, the difference value $\Delta\nu$ is a useful characteristic for determining the coordination mode of the carboxylate group of the ligands. The observed $\Delta\nu$ for Th(IV), Zr(IV), and V(IV) complexes (Table 3, Note 4. and 5.) fall in the range 196-202 cm^{-1} indicating a monodentate coordination mode of the carboxylato group (Dendrinou-Samara et al., 1998; Nakamoto, 1986) .

(v) The IR spectral data of the three complexes show medium-to-medium-weak bands around 3390 cm^{-1}, and weak to very weak band at 2933-2375, 2845-2356, and 2883-2344 for Th(IV), Zr(IV), and V(IV) complexes, respectively. These bands can be assigned to the vibrations of the quaternized nitrogen ($-^+NH_2$) of the piperazinyl group, which indicated that the zwitterionic form of NFX is involved in the coordination of the Th, Zr, and V ion investigated (Silverstein et al., 1991).

(vi) The vibrations of the free sulphate group in V(IV) complex, $[VO(NFX)_2]SO_4$, can be assigned as follows:

two weak intensities bands occur in the region above 1000 cm^{-1} at 1195 and 1036 cm^{-1}, are assigned to the different symmetric and antisymmetric bond vibrations, $\upsilon(SO_4^{2-})$, and medium strong band at 689 cm^{-1} is assigned to the bending motion of $\delta(SO_4^{2-})$.

(vii) The υ(V=O) stretching vibration in the vanadyl complex is observed as expected as a medium band at 956 cm^{-1}, which is a good agreement with those known for many dioxovanadium (IV) complexes.

According to the IR spectral data, the NFX is coordinated to the metal ions as a bidentate ligand via one-carboxylato oxygen atoms and the oxygen atom of the pyridine carbonyl group (Turel, 2002).

3.2 Electronic absorption spectra

Electronic spectra of the NFX complexes were recorded in the 200-800 nm region in DMSO (Fig. 4) There are two detected absorption bands at 285 and 335 nm in electronic spectrum of NFX, assigned to n-π* and π-π* transitions. These transitions occur in case of unsaturated hydrocarbons, which contain carbon atom attached with oxygen atoms as in carboxylic and ketone groups (Refat, 2007). The electronic spectra of Th(IV), Zr(IV), and V(IV) complexes show two absorption bands at 250 and 285 nm. The band at 335 nm is absent in the electronic spectra of the complexes which may indicate that the carboxylic group and ketone groups are involved in the complexation.

3.3 ^{1}H NMR spectra

The ^{1}H NMR spectral data of the $[Th(NFX)_2Cl_4]$ complexes and the free ligand (NFX) are represented in Table 4, and all assignments. The spectrum of the complex is shown in Fig. 5. The literature values of the ^{1}H NMR chemical shifts (δ, ppm) of NFX are included in Table 4 for comparison purposes. Upon comparison with the free ligand, the absent of the characteristic peak for hydrogen of –COOH at δ 11.00 ppm in Th(IV) complex indicates coordination of NFX ligand to Th(VI) through the deprotonated carboxylic group (Refat, 2007; Sadeek, 2005). The spectrum also show characteristic three peaks for quaternized nitrogen ($-^+NH_2$) at δ 2.10, 2.50, and 3.9 ppm (Sadeek et al., 2009). The broad peak at δ 3.9 ppm, which was not detected in the spectra of free NFX ligand, confirmed the deprotonation of the two –COOH groups in NFX. The overall changes of the ^{1}H NMR spectrum of the Th (IV) complex is indicative of coordination of NFX ligand to the metal via the pyridone and one carboxylate oxygen atoms (Riley et al., 1993). This suggested coordination is in agreement with that obtained by elemental analysis and IR spectra.

3.4 Thermogravimetric analysis

The Norfloxacin of T(IV), Zr(IV), and V(IV) complexes are stable at room temperature and can be stored for several months without any changes. The obtained complexes were studied by thermogravimetric (TG) and differential thermogravimetric (DTG) analysis from ambient temperature to 900 °C N_2 atmospheres. The TG curves were redrawn as mg mass loss versus temperature (TG) curves and as the rate of loss of mass versus temperature (DTG) curves. Typical TG and DTG curves are presented in Fig. 6, and the thermoanalytical results are summarized in Table 5. The overall loss of mass from the TG curves is 97.74% for NFX, 68.64% for $[Th(NFX)_2Cl_4]$, 86.28% for $[Zr(NFX)_2Cl_2]Cl_2$, and 85.12% for $[VO(NFX)_2]SO_4$. All the complexes show two or three stages of mass loss in their TG/DTG curves, and all mass loss in these stages is due to the decomposition of counter ions and NFX molecules.

3.4.1 Norfloxacin ligand

The data obtained indicate that the NFX is thermally stable in the temperature range 25-50 °C. Decomposition of NFX start at 50 °C and finished at 726 °C with three stages. The first stage of decomposition occurs between 25 and 270 °C, at maximum temperature of 125 °C, and is accompanied by weight loss of 8.38%, corresponding exactly to the loss of ethylene molecule (C_2H_2). The second stage of decomposition starts at 270 °C and end at 575 °C, showing an endothermic peak at 335 °C. This stage is accompanied by a weight loss of 69.80%, corresponding to the loss of $4C_2H_2 + HF + N_2 + CO + CO_2$. The final decomposition step occurs in the range 575-720 °C with a maximum at 650 °C, and is accompanied by a weight loss of 19.56%, and my be attributed to the loss of pyrrole ring, $2C_2H_2 + 1/2N_2$, $1/2H_2$, in reasonable agreement with the theoretical value of 21.0%.

3.4.2 $[Th(NFX)_2Cl_4]$ complex

The thermal decomposition of $[Th(NFX)_2Cl_4]$ complex proceeds approximately with three main degradation stages in 25-900 °C temperature range. The first stage of decomposition is exothermic stage occurs at three maximum temperature of 50, 108, and 218 °C, and is accompanied by a weight loss of 11.84%, corresponding to the loss of $2C_2H_2 + Cl_2$. The second stage of decomposition occurs at three maximum temperatures at 308, 377, and 455 °C. The weight loss in this step is 37.69%, corresponding to the loss of $5C_2H_2 + Cl_2 + 2HF + 2N_2 + 2NO$

+ 2CO. The final step is associated with the loss of $7C_2H_2$ + CO + $4H_2$ forming ThO_2 + 4C as a final product.

3.4.3 $[Zr(NFX)_2Cl_2]Cl_2$ complex

The thermal analysis curves of $[Zr(NFX)_2Cl_2]Cl_2$ complex show that decomposition takes places in two stages. The first stage is exothermic stage occurs at two maximum temperature at 60 and 298 °C. The broader exothermic peak at 60 °C indicate a slow in heat capacity (Shaikh et al., 2007). The weight loss in this stage is 17.61% in the 25-250 range corresponding to the loss of $2C_2H_2$ + $3/2Cl_2$. The following stage occurs at maximum temperature of 553 °C in the temperature range 250-900 corresponding to the formation of $13C_2H_2$ + $1/2Cl_2$ + 2HF + $2N_2$ + 2NO + 2CO + $2H_2$. The final thermal product obtained at 900 °C is ZrO_2.

3.4.4 $[VO(NFX)_2]SO_4$ complex

Thermal decomposition of $[VO(NFX)_2]SO_4$ proceeds in three stages. The first stage is occurs at maximum temperature at 60 °C (DTG), in the temperature range 25-210 °C. The mass loss in this stage is found to be 14.81%, corresponding to the thermal decomposition of the complex by the loss of $2C_2H_2$ + SO_2. This is followed by another mass loss (68.38%) in the temperature range 210-520 °C, by giving an endothermic effect (DTG_{max}, 260, 374, 445 °C). In the final stage, the complex decomposes in consecutive steps in the 520-900 °C temperature range to give $VO_{2.5}$ with some carbon atoms.

Reported data on thermal analysis studies in the nitrogen atmosphere indicate that the Th(IV), Zr(IV), V(IV) complexes decompose to give metal oxide as final product, with few carbon atoms (except Zr(IV) complex), indicates that no sufficiently of oxygen atoms helps to evolved carbon as carbon monoxide or dioxide. The found weight loss associated with each step of decomposition for each complex agrees well with the calculated weight loss (Table 5). The final products of the complexes obtained at 900 °C were confirmed with infrared spectra.

3.5 Kinetic parameters

Two methods of decomposition kinetics studies have been applied in this study; Coats-Redfern (Coats & Redfern, 1964) and Horowitz-Metzger (Horowitz & Metzger, 1963).

3.5.1 Coats-Redfern equation

The Coats-Redfern equation (1), which is atypical integral method, can be represented as:

$$\int d\alpha/(1-\alpha)^n = (A/\varphi)\int e^{-E^*/RT}\,dT \quad (1)$$

For convenience of integration, the lower limit T1 is usually taken as zero. This equation on integration gives:

$$ln\,[-ln\,(1-\alpha)/T^2] = -E^*/RT + ln\,[AR/\varphi E] \quad (2)$$

A plot of left-hand side (LHS) against 1/T was drawn. E^* is the energy of activation in KJ mol^{-1} and calculated from the slop and A in (s^{-1}) from the intercept. The entropy of activation ΔS^* in (JK^{-1} mol^{-1}) was calculated by using the equation:

$$\Delta S^* = Rln\,(Ah/kT_s) \quad (3)$$

where k is the Boltzmann constant, h is the Plank's constant and T_s is the DTG peak temperature.

3.5.2 Horowitz-Metzger equation

The Horowitz-Metzger (Eg. 4) was written in the form as follows:

$$log\,[log\,(w_\alpha/w_\gamma)] = E^*\,\theta/2.303RT_s^2 - log2.303 \quad (4)$$

Where $\theta = T - T_s$, $w_\gamma = w_\alpha - w$, w_α = mass loss at the completion of the reaction; w = mass loss up to time t.

The plot of $Log\,[log\,(w_\alpha/w_\gamma)]$ versus θ was drawn and found to be linear from the slope E^* was calculated. The pre-exponential factor, A, was calculated from the Eg. (5):

$$E^*\,\theta/RT_s^2 = A/[\varphi exp\,(-E^*/RT_s)] \quad (5)$$

From the TG curves, the activation energy, E^*, entropy of activations, ΔS^*, enthalpy activations, ΔH^*, and Gibbs free energy, ΔG^*, were calculate from;

$\Delta H^* = E^* - RT$ and $\Delta G^* = \Delta H^* - T\Delta S^*$

The linearization curves of Coats-Redfern and Horowitz-Metzger methods are shown in Fig 7. Kinetic parameters for the first stages, calculated by employing Coats-Redfern and Horowitz-Metzger equations, are summarized in Table 6 (Note 6.), together with the radii metal ions. The results show that the values obtained by various methods are comparable. The kinetic data obtained with the two methods are in harmony with each other. The activation energy of Th(IV), Zr(IV) and V(IV) complexes is expected increase in relation with decrease in

their radius (Avsar et al., 2002). The E^* values calculated with the method of Coats-Redfern for the first decomposition stage of the complexes are given below:

E^*V(IV) =1.73×10^5 kJmol^{-1} > E^*Zr(IV) =1.38×10^5 kJmol^{-1} > E^*Th(IV) = 8.19×10^4 kJmol^{-1}

rV(IV) = 72 pm < rZr(IV) = 86 pm < rTh(IV) = 108 pm

3.6 Antimicrobial activities

Applying the nutrient filter paper disc method, all of the newly synthesized NFX complexes and NFX were screened in vitro for antibacterial and antifungal activity. The activity was determined against three bacterial species, *Bacillus subtilis*, *Pseudomonas aeruginosa* (*P. aeuginosa*), and *Escherichia coli* (*E. coli*), and antifungal screening was studied against three species, *Aspergills flavus*, *Fusarium solani*, and *Penicillium verrcosum*. The activity was performed by measuring the diameter of the inhabitation zone, and the screening results are given in Table 7 (Note 7.). The results show that the metal complexes are more effective as antibacterial and antifungal agents as compared to the uncomplexed ligand. This increase in the activity is being considered due to increased bioavailability of the metal drug complexes and the aqueous solubility of NFX. Th(IV) complex exhibit higher activity than other complexes. All the three complexes exhibited no inhibitory activates against *Bacillus subtilis* species.

4. Conclusion

Transport of organic ligands into bacterial cells can be facilitated by the formation of metal complexes. Hence, Th(IV), Zr(IV) and V(IV) complexes of norfloxacin were synthesized. UV, IR, 1 H NMR, elemental analysis and thermogravimetric analysis (TG) and differential thermal analysis (DTG), characterized the isolated solid complexes. In all the complexes, norfloxacin is bound to the metal via the pyridone and one carboxylate oxygen atoms, and the complexes are found to possess metal to ligand ratio of 1:2. Antimicrobial studies were carried out against several types of bacteria and fungi. Th(IV), Zr(IV) and V(IV) complexes are found to possess better activity against all the microorganisms tested (except *Bacillus subtilis* species), than that of norfloxacin. It was concluded that the obtained complexes could be better alternative to norfloxacin as an antibacterial and antifungal agent.

Acknowledgements

The author is deeply grateful to the member staff of Department of Microbiology, Egyptian International Pharmaceutical Industrial Company (EIPICO), for performing the antimicrobial evaluation.

References

Al-Mustafa, J. (2002). Magnesium, calcium and barium perchlorate complexes of ciprofloxacin and norfloxacin. *Acta Chimica Slovenica*, *49,* 457-470.

Avsar, G., Kulcu, N., & Arslan, H. (2002). Thermal behavior of copper(II), nickel(II), cobalt(II) and palladium(II) complexes of N, N-dimethyl-N'-benzoylthiourea. *Turkish Journal of Chemistry*, *26,* 607-616.

Beecher, D. J., & Wong, A. C. (1994). Identification of hemolysin BL-producing Bacillus cereus isolates by a discontinuous hemolytic pattern in blood agar. *Applied and Environmental Microbiology*, *60,* 5, 1646-1651.

Chu, D. T. W., Fernandes, P. B., & Perent, A. G. (1986). Synthesis and biological activity of benzothiazolo [3, 2-a] quinolone antibacterial agents. *Journal of Medicinal Chemistry*, *29,* 1531. http://dx.doi.org/1021/jm00158a037

Coats, A. W., & Redfern, J. P. (1964). Kinetic Parameters from Thermogravimetric Data. *Nature, 201,* 68. http://dx.doi.org/10.1038/201068a0

Cui, J., Zhang, K., Huang, Q., Yu, Y., & Peng, X. (2011). An indirect competitive enzyme-linked immunosorbent assay for determination of norfloxacin in waters using a specific polyclonal antibody. A*nalytica Chimica Acta*, *688,* 84-89. http://dx.doi.org/10.1016/j.aca.2010.12.030

Deacon, G. B., & Phillips, R. J. (1980). Relationships between the carbon-oxygen stretching frequencies of carboxylato complexes and the type of carboxylate coordination. *Coordination Chemistry Reviews*, *33,* 227-250. http://dx.doi.org/10.1016/S0010-8545(00)80455-5

Dendrinou-Samara, C., Tsotsou, G., Ekateriniadou, L. V., Kortsaris, A. H., Raptopoulou, C. P., Terzis, A., Kyriakidis, D. A., & Kessissoglou, D. P. (1998). Anti-inflammatory drugs interacting with Zn(II), Cd(II) and Pt(II) metal ions. *Journal of Inorganic Biochemistry*, *71,* 171-179.

Dhaneshwar, S., Tewari, K., Joshi, S., Godbole, D., & Ghosh, P. (2001). Diglyceride prod rug strategy for

enhancing the bioavailability of norfloxacin. *Chemistry and Physics of Lipids*, *164,* 307-313. http://dx.doi.org/10.1016/j.chemphyslip.2011.03.006

Domagala, J. M., Heifetz, C. L., Hutt, M. P., Mich, T. F., Nichols, J. B., Solomon, M., & Worth, D. F. (1988). 1-Substituted 7-[3-ethylamino) methyl] -1- pyrrolidinyl] -6,8-difluoro -1,4-dihydro -4- oxo -3-quindine carboxylic acids. New quantitative structure activity relationships at N1 for the quinolone antibacterials. *Journal of Medicinal Chemistry*, *31,* 991-1001. http://dx.doi.org/10.1021/jm00400a017

Efthimiadou, E. K., Psomas, G., Sanakis, Y., Katsaros, N., & Karaliota, A. (2007). Metal complexes with the quinolone antibacterial agent *N*-propyl-norfloxacin: Synthesis, structure and bioactivity. *Journal of Inorganic Biochemistry*, *101,* 525-535. http://dx.doi.org/10.1016/j.jinorgbio.2006.11.020

Fang, K. -C., Chen, Y. -L., Sheu, J. -Y, Wang, T. -C, & Tzeng, C. -C. (2000). Synthesis, Antibacterial, and Cytotoxic Evaluation of certain 7-substitued Norfloxacin Derivatives. *Journal of Medicinal Chemistry*, *43,* 3809-3812. http://dx.doi.org/10.1021/jm000153x

Horowitz, H. H., & Metzger, G. (1963). A New Analysis of Thermogravimetric Traces. *Analytical Chemistry, 35,* 1464-1468. http://dx.doi.org/10.1021/ac60203a013

Koga, H., Itoh, A., Murayama, S., Suzue, S., & Irikura, T. (1980). Structure-activity relationships of antibacterial 6, 7-and, 8-disubstituted 1-alkyl-1, 4-dihydro-4-oxoquinoline-3-carboxylic acids. *Journal of Medicinal Chemistry*, *23,* 1358-1363. http://dx.doi.org/10.1021/jm00186a014

Nakamoto, K. (1986). *Infrared and Ramman Spectra of Inorganic and Coordination Compounds*. (4th ed.). New York: Wiley. pp. 230.

Naumann, P., & Dopp, C. (1989). Fluoroquinolones-antibacterial activity, pharmacokinetics and indications for a new group of chemotherapeutic drugs. *Internist* (Berl.) *30,* 20-31.

Polk, R. E., & Pharm, D. (1989). Drug-drug interactions with ciprofloxacin and other fluoroquinolones. *The American Journal of Medicine*, *87,* 76-81. http://dx.doi.org/10.1016/0002-9343 (89)90028-4

Refat, M. S. (2007). Synthesis and characterization of norfloxacin-transition metal complexes (group 11, IB): Spectroscopic, thermal, kinetic measurements and biological activity. *Spectrochimica Acta Part A*, *68,* 1393-1405. http://dx.doi.org /10.1016/j.saa.2006.12.078

Reynolds, J. E. (Ed.), (1993). *Martindale: The Extra Pharmacopeia*. (30rd ed.). London: Pharmaceutical Press, pp. 145-147.

Riley, C. M., Ross, D. L., van der Velde, D., & Takusagawa, F. (1993). Characterization of the complexation of fluoroquinolone antimicrobials with metal ions by nuclear magnetic resonance spectroscopy. *Journal of Pharmaceutical and Biomedical Analysis*, *11,* 49-59. http://dx.doi.org/doi: 10.1016/0731-7085(93)80148-T

Sadeek, S. A. (2005). Synthesis, thermogravimetric analysis, infrared, electronic and mass spectra of Mn(II), Co(II) and Fe(III) norfloxacin complexes. *Journal of Molecular Structure*, *753,* 1-12. http://dx.doi.org/10.1016/j.molstruc.2005.06.011

Sadeek, S. A., El-Did Amony, A. M., El-Shwiniy, W. H., & Zordok, W. A. (2009). Uranium (VI) and zirconium (IV) of the second-generation quinolone antimicrobial drug norfloxacin: Structure and biological activity. *The Journal of Argentine Chemical Society*, *97,* 2, 51-76.

Sadeek, S., A., El-Shwiniy, W., H., Zordok, W., A., & El-Didamony, A., M. (2009). Synthesis, spectroscopic, thermal and biological activity investigation of new Y(III) and Pd(II) norfloxacin complexes. *The Journal of the Argentine Chemical Society*, *97,* 2, 128-148.

Sadeek, S. A., Refat, M. S., & Hashem, H. A. (2006). Complexation and thermogravimetric investigation on tin(II) and tin(IV) with norfloxacin as antibacterial agent. *Journal of Coordination Chemistry*, *7,* 759-775. http://dx.doi.org/10.1080/00958970500404534

Shaikh, A. R., Giridhar, R., & Yadav, M. R. (2007). Bismuth-norfloxacin complex: Synthesis, physicochemical and antimicrobial evaluation. *International Journal of Pharmaceutics*, *332,* 24-30. http://dx.doi.org/10.1016/j.ijpharm.2006.11.037

Silverstein, R. M., Bassler, G., C., & Morril, T. C. (1991). *Spectroscopic Identification of Organic Compounds*, (5th ed.). New York: Wiley.

Sunduru, N., Gupta, L., Chauhan, K., Mishra, N. N., & Shukla, P. K. (2011). Synthesis and antibacterial evaluation of novel 8-fluoro Norfloxacin derivatives as potential probes for methicillin and vancomycin-resistant

Staphylococcus aureus. *European Journal of Medicinal Chemistry*, *46,* 1232-1244. http://dx.doi.org/10.1016/j.ejmech.2011.01.044

Turel, I. (2002). The interaction of metal ions with quinolone antibacterial agents. *Coordination Chemistry Reviews*, *232,* 27-47.

Turel, I., Leban, I., & Bukovec, N. (1997a). Crystal Structure and Characterization of the Bismuth (III) Compound with Quinolone Family Member (Ciprofloxacin), Antibacterial Study. *Journal of Inorganic Biochemistry*, *66,* 241-245.

Turel, I., Bukovec, P., & Quirós, M. (1997b). Crystal structure of ciprofloxacin hexahydrate and its characterization. *International Journal of Pharmaceutics*, *152,* 59-65.

Turel, I., Golic, L., Bukovec, P., & Gubina, M. (1998). Antibacterial tests of Bismuth (III)-Quinolone (Ciprofloxacin, cf) compounds against *Helicobacter pylori* and some other bacteria. Crystal structure of $(cfH_2)_2[Bi_2Cl_{10}].4H_2O$. *Journal of Inorganic Biochemistry*, *71,* 43-60.

Wu, G., Wang, G., Fu, X., & Zhu, L. (2003). Synthesis, Crystal Structure, Stacking Effect and Antibacterial Studies of a Novel Quaternary Copper (II) Complex with Quinolone *Molecules*, *8,* 287-296. http://dx.doi.org/10.3390/80200287

Notes

Note 1. Measured in 10^{-3} M DMSO solutions at room temperature.

Note 2. s =strong, w = weak, m = medium, sh = shoulder, v = very, br= broad

Note 3. υ, stretching;δ, bending.

Note 4. $\Delta\nu = \nu_{as}(COO^-) - \nu_s(COO^-)$.

Note 5. As ν(COOH).

Note 6. Units of parameters: *E* in kJ mol^{-1}, *A* in s^{-1}, *ΔS* in J $mol^{-1}K^{-1}$, *ΔH* and *ΔG* in kJ mol^{-1}.

Note 7. (-) NO activity, (+) mild activity, (++) moderate activity, (+++) marked activity, (++++) strong marked activity.

Table 1. Elemental analysis and physical properties of the compounds

Compound	Molecular weight	Yield (%)	Color	mp (°C)	Analysis (%) found (calculated)					$\Lambda^{Note\ 1.}$ ($\Omega^{-1}cm^2mol^{-1}$)
					C	H	N	Cl	M	
NFX, $C_{16}H_{18}FN_3O_3$	319	-	Yellow	232	59.45 (60.18)	5.54 (5.68)	12.89 (13.16)	-	-	10.16
$[Th(NFX)_2Cl_4]$	1012	74	White	> 300	37.96 (37.94)	3.58 (3.56)	8.30 (8.30)	14.01 (14.03)	22.92 (22.92)	85.00
$[Zr(NFX)_2Cl_2]Cl_2$	871.23	76	White	> 300	44.09 (44.08)	4.16 (4.13)	9.64 (9.64)	16.27 (16.30)	10.47 (10.47)	73.00
$[VO(NFX)_2]SO_4$	810	73	Greenish brown	> 300	47.64 (47.40)	4.53 (4.45)	10.48 (10.37)	-	7.41 (6.95)	87.20

Table 2. IR frequencies[Note 2.] (cm^{-1}) and tentative assignments[Note 3.] for: NFX and Th(IV), Zr(IV), and V(IV) compounds

NFX	Th(IV)	Zr(IV)	V(IV)	Assignments
3399ms	3390m, br	3903w, 3715w, 3396m, br	3685w, 3435m, 3317m	υ(N-H)+υ_{as}(O-H);H_2O
3267vw, 3228vw, 3189vw, 3130vw, 3021w, 2927m, 2823w, 2796w, 2764w, 2723m, 2696vw, 2654w, 2617w, 2511w, 2468m	3253m, 3120vw, 2933vw, 2791vw, 2375w, 2348vw	2988vw, 2845vw, 2356m, 2320 mw	2967vw, 2883vw, 2817vw, 2344m, 2314m, sh	υ_s(O-H);H_2O,υ(C-H),υ(N-H),υ(-NH_2^+)
1727sh, 1716ms	1688 m	1679w	1657 w	υ(C=O):(COOH)
1630vs, 1552w	1617 m, 1576 s	1610vs, 1579vs	1615 ms, 1583s	υ(C=O)+δ_b(H_2O) phenyl breathing modes
1482vs, 1454m	1495vs, 1458m	1477m, 1447m	1497vs,	CH: deformation of -CH_2
1396s	1385s, 1355m	1387s, 1361m	1381vs, 1358s	υ_s(COO^-) + υ(N-O): NO_3^-
1307 vw	1310m	1317 m	-	δ_b(CH_2)
1277vw, 1263s, 1248vw	1245vw	1285 m	1252 ms	υ(C-C)
1201m, 1192m	1207vw	1188 w	1195 w	υ(C-O) υ(C-N)
1153vw, 1142w, 1132w, 1115w, 1095m, 1076m, 1051vw, 1036ms, 1024w, 1005 m, 982 m	1151 w, 1091w 1068w	1144 vw	1036 vw	δ_r(CH_2)
750s, 706m	760m, 718m	763m, 705m	776m, 727w	δ_b(COO^-)
667w, 631w, br, 569ms, 524w, 499m, 474m, 453vw, 430ms	679w, 645w, 502w, 471vw	651mw, 627vw, 563m, 531 vw, 489 w, 465 w	689ms, 641w, 579w, 546w, 503vw, 491w, 466vw	υ(M-O) + ring deformation

Table 3. Characteristic absorptions of carboxylate group (in cm^{-1}) and $\Delta\nu$ values

Compound	$\nu(C=O)_p$	$\nu(COO^-)_{asym}$	$\nu(COO^-)_{sym}$	$\Delta\nu$ [Note 4.]
NFX	1630	1727 [Note 5.]	-	-
$[Th(NFX)_2Cl_4]$	1617	1576	1380	196
$[Zr(NFX)_2Cl_2]Cl_2$	1610	1579	1382	197
$[VO(NFX)_2]SO_4$	1615	1583	1381	202

Table 4. ^1H NMR spectral data of free NFX and $[Th(NFX)_2Cl_4]$ complex

NFX	$[Th(NFX)_2Cl_4]$	Assignments
1.13	1.70	δ H, -CH_3
2.0	2.10	δ H, -NH; piperazine
-	2.50	δ H, -$^+NH_2$
-	3.9	δ H, -$^+NH_2$
2.78, 3.10, 3.47	-	δ H, -CH_2; piperazine δH, -CH_2; -CH_2CH_3
5.93, 7.12, 8.01	7.2, 7.3, 7.7, 8.1, 8.2, 8.3	δ H, -CH aromatic
11.00	8.8	δ H, -COOH

Table 5. Thermo analytical results for the investigated compounds

Samples	Stage	TG results temp. peak (°C)	DTG results temp. range (°C)	Weight loss (%)		Evolved moiety
				Found	Calcul-ated	
NFX	I	25-270	125	8.38	8.78	C_2H_4
($C_{16}H_{18}N_3$	II	270-575	335	69.80	70.22	$HF + 4C_2H_2 + CO + CO_2 + N_2$
O_3F)	III	575-726	650	19.56	21.00	$2C_2H_2 + 0.5H_2 + 0.5N_2$
Th/NFX	I	25-260	50, 108, 218	11.84	12.15	$2C_2H_2 + Cl_2$
($C_{32}H_{36}N_6$	II	260-530	308, 377, 455	37.69	38.04	$5C_2H_2 + Cl_2 + 2HF + 2N_2 + 2NO + CO$
O_6FCl_4)Th	III	530-900	580	19.11	18.97	$7C_2H_2 + CO + 4H_2$
	Residue			31.36	30.83	$ThO_2 + 4C$
Zr/NFX	I	25-250	60, 298	17.61	18.19	$2C_2H_2 + 3/2Cl_2$
($C_{32}H_{36}N_6$	II	250-900	553	68.67	67.66	$13C_2H_2 + 1/2Cl_2 + 2HF + 2N_2 + 2NO + 2CO + 2H_2$
O_6FCl_4)Zr	Residue			13.71	14.14	ZrO_2
V/NFX	I	25-210	60	15.06	14.81	$2C_2H_2 + SO_2$
($C_{32}H_{36}N_6$	II	210-520	260	68.38	68.15	$12C_2H_2 + 2HF + 2N_2 + 2NO + CO + 1/2CO_2 + O_2$
$O_{10}FS$)V	III	520-900	374, 445	1.68	1.73	$1/2CO$
	Residue			14.88	15.31	$VO_{2.5} + 2C$

Table 6. Thermal behavior and kinetic parameters determined using the Coats-Redfern (CR) and Horowitz-Metzger ((HM)

Compounds	Radius metal ion/pm	T_s (K)	Method	Parameters Note 6.					
				E^*	A	ΔS^*	ΔH^*	ΔG^*	r
NFX (16)	-	-	CR	9.36×10^4	2.00×10^1	-5.01×10^1	9.03×10^4	1.10×10^5	0.9853
			HM	9.66×10^4	8.68×10^1	-3.79×10^1	9.33×10^4	1.08×10^5	0.9817
Th / NFX	108	550	CR	8.19×10^4	1.26×10^6	-1.37×10^2	1.31×10^5	2.44×10^5	0.9855
			HM	1.46×10^5	1.23×10^7	-1.18×10^2	1.39×10^5	2.36×10^5	0.9777
Zr/NFX	86	344	CR	1.38×10^5	3.59×10^4	-1.64×10^2	7.67×10^4	1.78×10^5	0.9812
			HM	8.82×10^4	2.02×10^5	-1.49×10^2	8.30×10^4	1.75×10^5	0.9806
V/NFX	72	377	CR	1.73×10^5	7.53×10^{11}	-2.40×10^1	1.67×10^5	1.83×10^5	0.9980
			HM	1.93×10^5	4.64×10^{13}	1.02×10^1	1.88×10^5	1.81×10^5	0.9955

Table 7. Antibacterial and antifungal activities [Note 7.] data for NFX and its compounds

Compound	Microbial species					
	Bacteria			Fungi		
	Bacillus subtilis	*P. aeruginosa*	*E. coli*	*Aspergills flavus*	*Fusarium solani*	*Penicillium verrcosum*
NFX	++++	+	-	-	-	++
$[Th(NFX)_2Cl_4]$	-	++++	++++	++	++++	++
$[Zr(NFX)_2Cl_2]Cl_2$	-	++	+++	+	++++	+
$[VO(NFX)_2]SO_4$	-	++	+++	+++	++	+++
Control (DMSO)	-	-	-	-	-	-

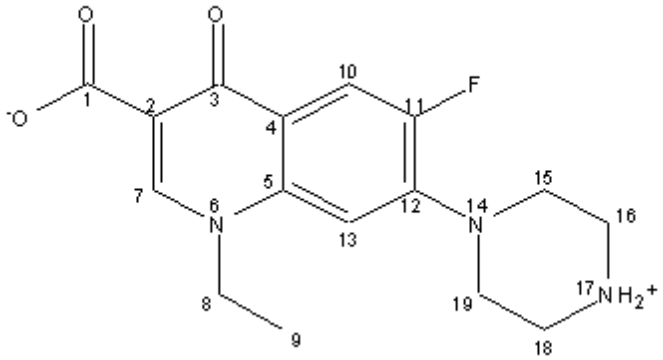

Figure 1. Structure of Norfloxacin (NFX) and its zwitterionic structure

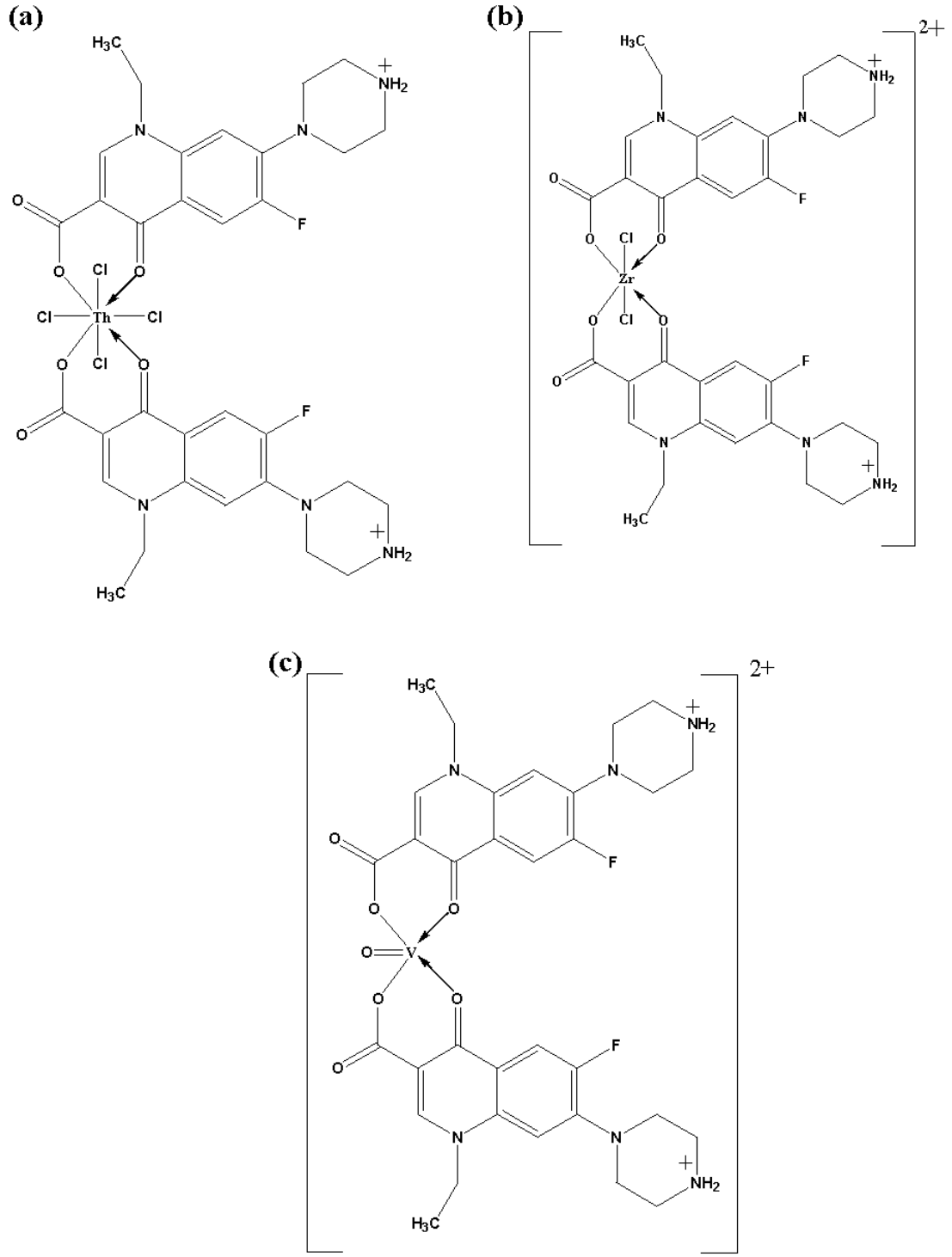

Figure 2. Suggested structure of (a) Th(IV), (b) Zr(IV), and (c) V(IV) – NFX complexes

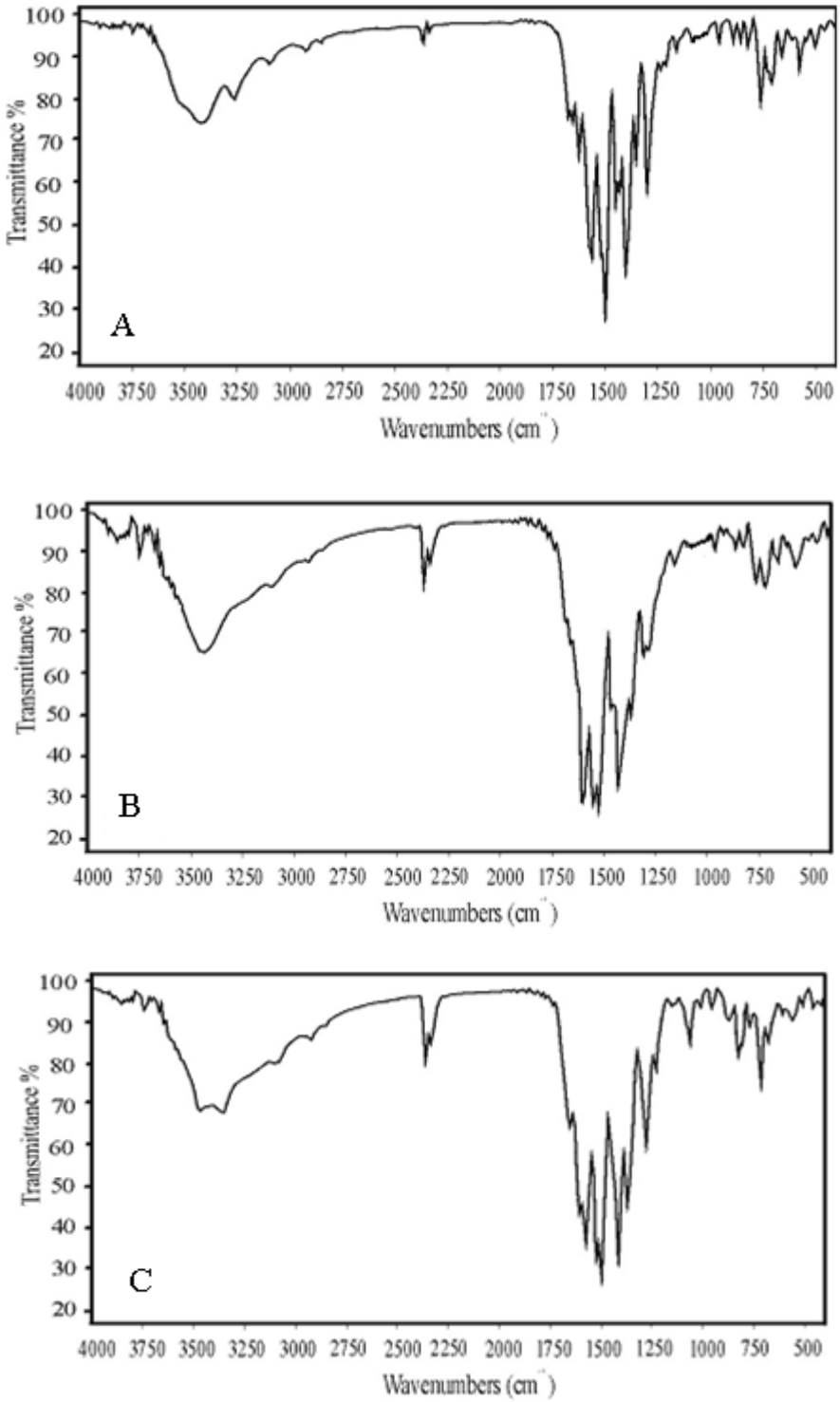

Figure 3. Infrared spectra of: (A) $[Th(NFX)_2Cl_4]$ complex; (B) $[Zr(NFX)_2Cl_2]Cl_2$ complex; (C) $[VO(NFX)_2]SO_4$ complex

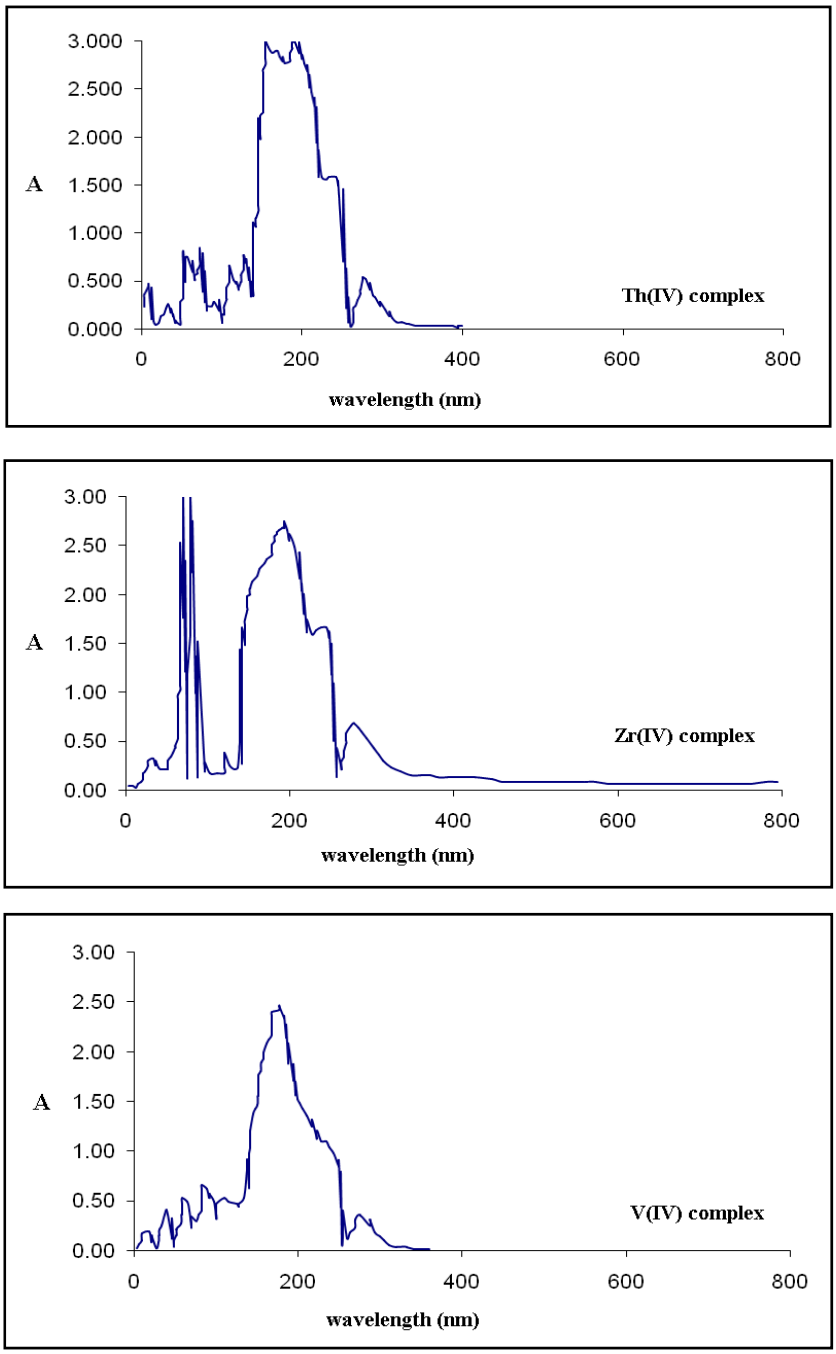

Figure 4. Electronic spectra of norfloxacin complexes

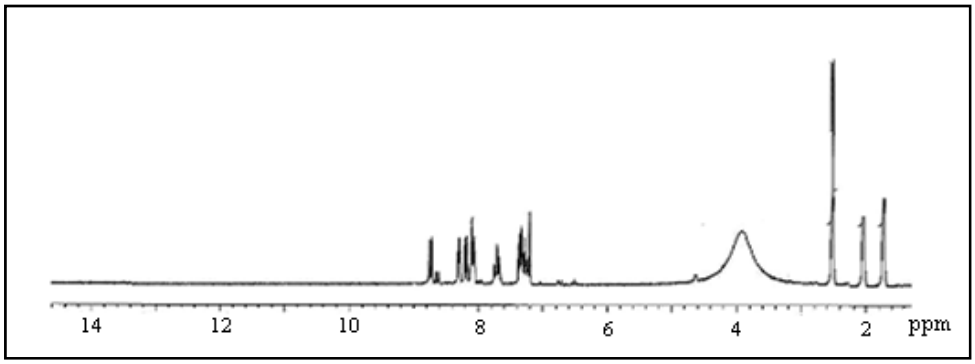

Figure 5. ^{1}H NMR spectra of $[Th(NFX)_2Cl_2]$ complex

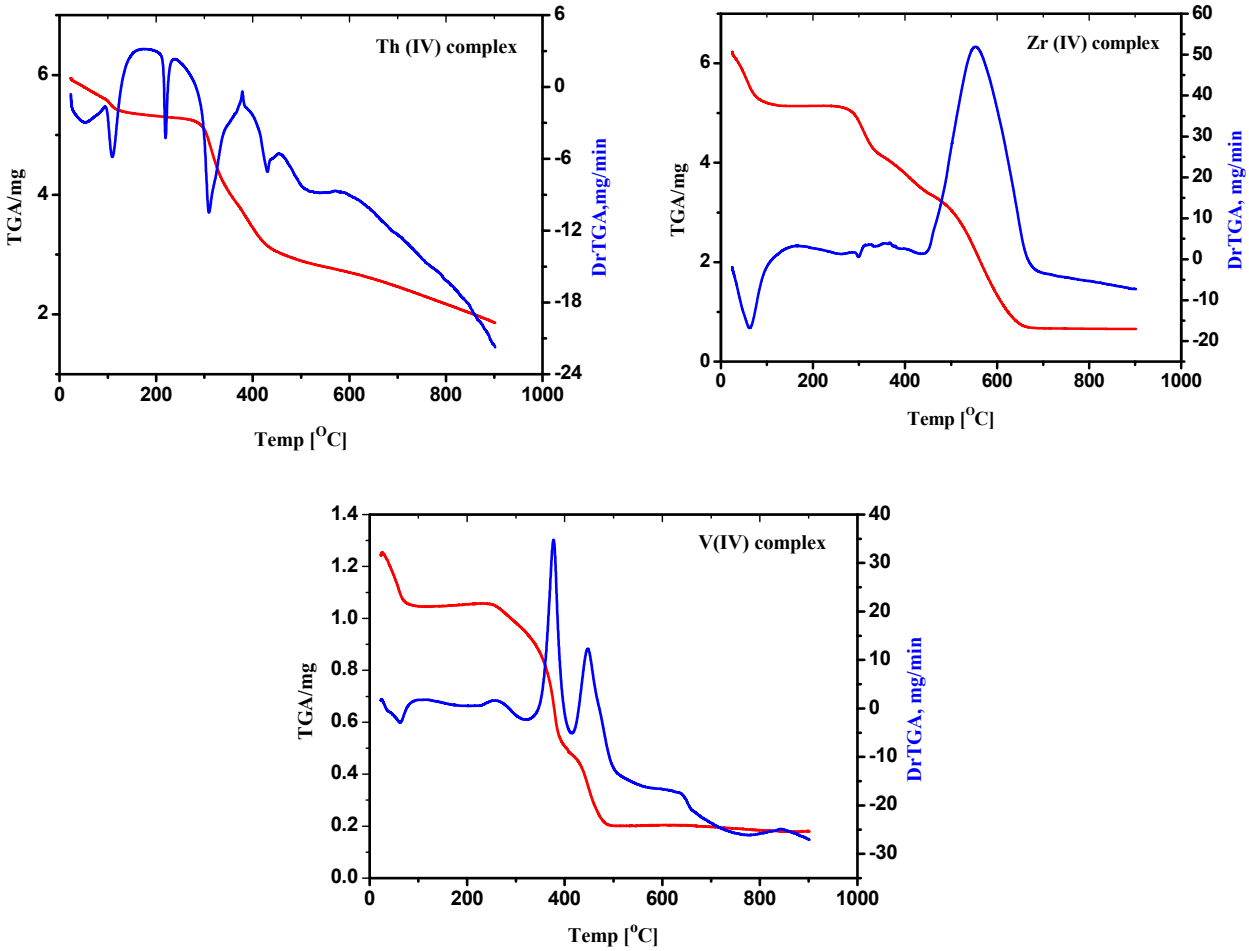

Figure 6. TG and DTG curves of Norfloxacin complexes

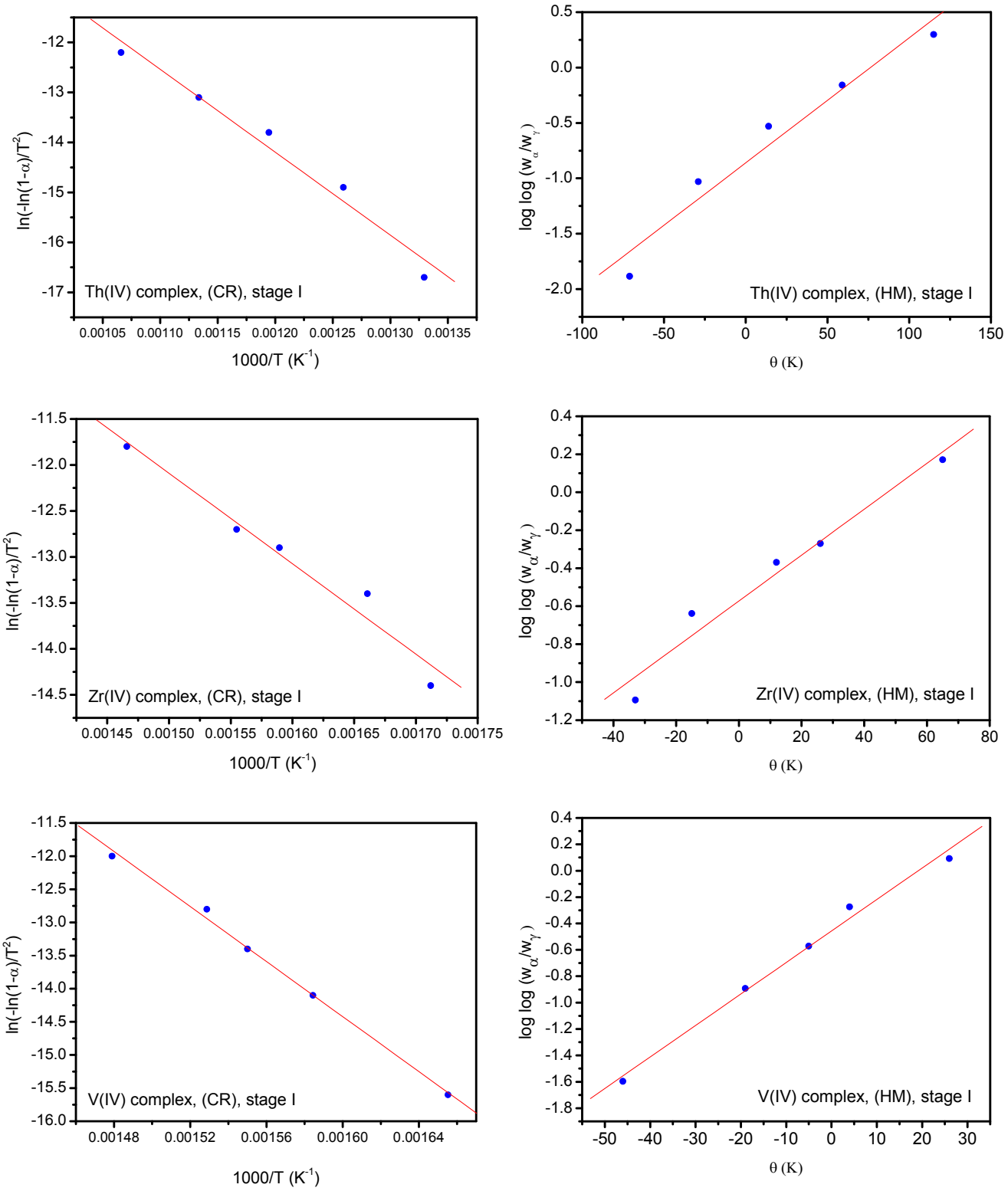

Figure 7. The diagrams of kinetic parameters of NFX complexes using Coats-Redfern (CR) and Horowitz-Metzger (HM) equations